



## OPEN Thinning altered the optimum photosynthetic environment in a subtropical coniferous plantation

Shengtong Li<sup>1</sup>, Mingjie Xu<sup>1,2</sup>, Fengting Yang<sup>2</sup>, Jiaxin Song<sup>1</sup>, Xinyi Shi<sup>1</sup>, Ziyi Wang<sup>1</sup>, Huimin Wang<sup>2,3</sup>, Xianjin Zhu<sup>1</sup>, Chuanpeng Cheng<sup>4</sup>, Jianlei Wang<sup>5</sup> & Tao Zhang<sup>1</sup>

Thinning offers long-term benefits for planted forests and is an important silvicultural practice. Meanwhile, ecosystem would respond to thinning and the optimal photosynthetic environment would change. Clarifying and quantifying the changing optimal photosynthetic environment induced by thinning is important for accurate prediction of carbon budgets and effective management of artificial forests. Based on six-year continuous in situ observations of carbon fluxes and corresponding environmental factors before and after 25% thinning in a typical subtropical plantation in China, this study revealed that thinning increased the optimum values of key environmental factors (net radiation (Rn), air temperature (Ta), and vapor pressure deficit (VPD)) for gross primary productivity (GPP). Meanwhile, thinning enhanced the ecosystem maximum GPP ( $GPP_{max}$ ) corresponding to each single optimum environmental factor. Among them, the highest  $GPP_{max}$  reaching  $0.91 \text{ mg CO}_2 \text{ m}^{-2} \text{ s}^{-1}$ , was found when Rn reached the optimum value and was 13% higher than that before thinning. In addition, the optimum photosynthetic environment configurations (the combination of multiple environmental factors) that could occur in the real world were detected and quantified. Before thinning, the optimal environment configuration was  $Rn = 692.85 \text{ J m}^{-2} \text{ s}^{-1}$ ,  $Ta = 23.43 \text{ }^\circ\text{C}$ ,  $VPD = 0.96 \text{ kPa}$  and  $SWC = 0.20 \text{ m}^3 \text{ m}^{-3}$ , with a  $GPP_{max}$  of  $0.98 \text{ mg CO}_2 \text{ m}^{-2} \text{ s}^{-1}$ . After thinning, the  $GPP_{max}$  increased to  $1.11 \text{ mg CO}_2 \text{ m}^{-2} \text{ s}^{-1}$ , and the corresponding optimal photosynthetic environment configuration was  $Rn = 693.92 \text{ J m}^{-2} \text{ s}^{-1}$ ,  $Ta = 26.70 \text{ }^\circ\text{C}$ ,  $VPD = 1.10 \text{ kPa}$  and  $SWC = 0.21 \text{ m}^3 \text{ m}^{-3}$ . All the values increased after thinning compared with those before thinning, and the changes in the optimal photosynthetic environment might be an important reason for the enhanced photosynthetic capacity of the thinned forests. These results indicated the positive responses of forest to proper thinning and could provide references for the development of forest management policies.

**Keywords** Thinning, Forest, GPP, Optimum environment, Eddy covariance

Forests, as the most important terrestrial carbon sinks, have received increasing attention because of their role in mitigating climate change, and artificial forests are being planted worldwide<sup>1</sup>. Thinning is an important silvicultural measure for planted forests. Accompanying climate change, air temperature (Ta) is increasing<sup>2,3</sup>, and precipitation patterns are changing and are predicted to induce more frequent droughts<sup>4-6</sup>. Changes in environmental factors together with anthropologic management or disturbances would greatly affect the photosynthetic capacity of forests<sup>7-9</sup>. Therefore, it is important to clarify the optimum photosynthetic environment for forests, which could be important indicators for predicting and estimating the carbon sink function of forests.

The response of forest photosynthesis to environmental factors is expected to follow the general response pattern of individual plants, with an “increase-peak-decrease” pattern. Insufficient light probably constrains photosynthesis<sup>10</sup>, whereas excessive radiation can lead to photoinhibition<sup>11</sup>. Low temperatures may reduce enzyme activity, whereas high temperatures can cause enzyme deactivation<sup>12</sup>. Water deficiency would lead to stomatal closure<sup>13</sup>, and excessive water would result in root hypoxia<sup>14</sup>. In essence, for each environmental

<sup>1</sup>College of Agronomy, Shenyang Agricultural University, Shenyang 110866, China. <sup>2</sup>National Critical Zone Observatory of Red Soil Hilly Region in Qianyanzhou, Key Laboratory of Ecosystem Network Observation and Modeling, Institute of Geographic Sciences and Natural Resources Research, Chinese Academy of Sciences, Beijing 100101, China. <sup>3</sup>University of Chinese Academy of Sciences, Beijing 100049, China. <sup>4</sup>College of Resources and Environment, Henan University of Economics and Law, Zhengzhou 450046, China. <sup>5</sup>China Nonferrous Metals Industry Technology Development and Exchange Center Co. Ltd, Beijing 100814, China. ✉email: xumj@syau.edu.cn; wanghm@igsnr.ac.cn; zhangt@syau.edu.cn

factor, there may exist an optimal value that maximizes ecosystem gross primary productivity (GPP). When an environmental factor deviates from its favorable range, either too high or too low, it will suppress GPP.

Previous studies have investigated the optimal  $T_a$  and optimal vapor pressure deficit (VPD) for forest photosynthesis at the leaf, canopy, and ecosystem scales<sup>15–17</sup>. However, these studies focused on the responses of ecosystems to a given environmental factor<sup>18</sup>. In reality, the photosynthetic response of forests is the result of the synergistic effects of multiple environmental factors, including light, temperature, and water availability<sup>19</sup>. When one environmental factor reaches its theoretical optimum, constraints imposed by other factors may lead to a significant reduction in actual GPP relative to expected levels<sup>20</sup>. Consequently, the optimum environment configuration (the combination of multiple factors) may not equal the theoretical optimum value detected for each single factor. The deviation of the optimal photosynthetic environment configuration from the optima of each single factor may arise from the interdependencies among environmental factors<sup>13,21</sup>, which should be considered when studies are conducted in real-world ecosystems. For example, subtropical China is under the control of a subtropical high-pressure system, which results in strong radiation, high  $T_a$ , a shortage of precipitation (PPT) and thus high VPD in summer<sup>22</sup>. These climatic conditions can markedly reduce plant stomatal conductance and substantially impair photosynthetic efficiency<sup>23</sup>. This implies that even when  $T_a$  reaches its optimal value in summer, the elevated VPD may still constrain vegetation photosynthesis, thereby preventing GPP from achieving its theoretical maximum. Consequently, relying solely on the optimal value of a single environmental factor is insufficient for accurately capturing the actual photosynthetic potential of forest ecosystems. It is essential to comprehensively evaluate the combined effects of multiple environmental factors, i.e., the optimal photosynthetic environment configuration<sup>24</sup>.

To enhance terrestrial carbon sinks and safeguard the ecological environment, extensive planted forests have been established across China since the 1980s<sup>25</sup>. However, most artificial forests are pure forests. After decades of growth, many problems have emerged<sup>26,27</sup>. Especially, owing to the single tree species and lower biodiversity, the resistance of artificial forests to natural disasters, pests and diseases is usually weak, accompanied by greater ecological risks<sup>28,29</sup>. Thinning is considered an inevitable approach to reconstruct artificial forests, which have long-term ecological and economic benefits<sup>30,31</sup>. Therefore, it is important to clarify the effects of thinning on the optimum photosynthetic environment; thus, researchers could accurately predict the changing carbon sink function of artificial forests.

Thinning could greatly affect the microclimate in forests<sup>32,33</sup>. After thinning, the leaf area index (LAI) decreases, and the removal of trees creates canopy gaps. Hence, light transmittance increases, which subsequently leads to the redistribution of light and heat resources in both the canopy and understory layers<sup>34–36</sup>. Simultaneously, reduced canopy interception enables more precipitation to reach the ground, thereby effectively alleviating water competition among plants<sup>37</sup>. Furthermore, thinning influences other environmental factors, such as wind speed, soil temperature, and soil water content (SWC)<sup>38</sup>. These changes in environmental factors likely promote adaptive adjustments in both trees and understory vegetation, enabling them to fully exploit the altered microclimatic conditions. Forrester et al.<sup>39</sup> reported that thinning substantially increased the light use efficiency of individual trees, thereby improving the photosynthetic capacity of the remaining trees. Martin-Benito et al.<sup>40</sup> reported that improved soil moisture conditions and increased stomatal conductance after thinning significantly increased the intrinsic water use efficiency of European black pine plantations, increasing their resilience to climate change. According to previous studies, thinning would probably alter the response characteristics of forests to environmental factors and their resource utilization strategies. The optimal range of these factors for forests inevitably shifts as habitat changes, affecting tree photosynthetic physiological processes and ultimately influencing ecosystem productivity<sup>9,16</sup>. The optimal photosynthetic environment involves complex interactions and mutual constraints among various environmental factors, thinning may alter the pre-existing synergistic relationships among these environmental factors and redefine the optimal environment for photosynthesis. Thus, the impact of thinning on the optimum photosynthetic environment may be more intricate and challenging to predict<sup>13,21</sup>.

Previous studies have focused on the impacts of thinning on environmental conditions or the functions of ecosystems<sup>28,30</sup>. However, few studies have explored the optimal environment configuration for GPP and clarified the effects of thinning on the optimum environment. Therefore, we conducted this study in a typical subtropical coniferous plantation in southern China, a region characterized by extensive planted forests and great contributions to the terrestrial carbon sink. In detail, this study aimed to (1) quantify the theoretical optimum values of each key environmental factor for pre- and post-thinning, such as net radiation ( $R_n$ ), air temperature ( $T_a$ ), and water conditions (atmospheric water conditions represented by the vapor pressure deficit (VPD) and soil water conditions represented by the soil water content (SWC)) at the ecosystem scale; (2) identify the optimum photosynthetic environment configuration (the synergistic combination of  $R_n$ ,  $T_a$ , and VPD) that maximizes GPP under realistic conditions for pre- and post-thinning; and (3) determine the quantitative changes in this optimum environment configuration and the corresponding changes in  $GPP_{max}$  induced by thinning. This study would help elucidate the underlying mechanisms of the effects of thinning on forest photosynthetic capacity, thereby providing a theoretical foundation and practical guidance for the management of subtropical artificial forests and the enhancement of their carbon sink function.

## Materials and methods

### Site description

This study was conducted at the National Qianyanzhou Critical Zone Observatory of the Red Soil Hilly Region (QYZ for short) (26°44′29″N, 115°03′29″E, 102 m above sea level), which is located in a typical red soil hilly region in Jiangxi Province, China. It serves as a standard observation site within the China Flux Observation and Research Network (ChinaFLUX), featuring two forest flux towers—one established in 2002 and the other in 2008. QYZ is under the control of a typical subtropical monsoon climate. According to meteorological

observations at QYZ from 1985 to 2014, the mean annual temperature is  $18.0 \pm 0.4$  °C, and the mean annual precipitation is  $1464.5 \pm 308.8$  mm. There are four seasons: spring (March–May), summer (June–August), autumn (September–November) and winter (December–February).

The vegetation at this site is a typical subtropical coniferous plantation. Before 1983, this region experienced severe soil and water erosion. To address this situation, trees were planted in approximately 1985, with pioneer and fast-growing species of Masson pine (*Pinus massoniana* Lamb.), Slash pine (*Pinus elliottii* Englem.) and Chinese fir (*Cunninghamia lanceolata* Hook.)<sup>41</sup>. The ecological environment has recovered and improved since then and has been a model of ecological restoration. However, after years of development, pure forests face many ecological risks, and proper forest management measures are needed to address this issue.

### Thinning treatment

The coniferous trees at the QYZ station were planted with a high density of 1460 stems  $\text{ha}^{-1}$  in 1985. Therefore, many trees were suppressed and relatively small before thinning was conducted. To reconstruct and further improve the forest, the QYZ station conducted relatively large-scale thinning ( $\sim 40$  ha) in the winter of 2012 around the second flux tower ( $26^{\circ}45'03.01''\text{N}$ ,  $115^{\circ}03'36.24''\text{E}$ ) established in 2008. For study purposes, pre-thinning observations were conducted from 2009 to 2012, which could be used as the reference for studying the effects of thinning. Given that forests change very quickly after thinning, to study thinning effects, observations from 2013 to 2014 were studied as post-thinning. In the thinned regions around the flux tower, Masson pine was the overwhelmingly dominant species, accounting for more than 85% of all the trees<sup>42</sup>. Other species, including Slash pine, Chinese fir and naturally growing broadleaf trees such as *Schima superba*, *Liquidambar formosana*, and *Quercus acutissima*, together account for less than 15% of the forests.

When thinning was conducted, approximately 25% of the basal area was removed. This intensity represents a moderately intensive thinning approach widely adopted in the management of subtropical planted forests in China. The commercially valuable parts (timbers) of the tree trunks were removed from the site, and most of the slash was left on the site. Tree stumps were also retained on site, with heights typically ranging from 25 to 35 cm. To study the effects of thinning on forests, some plots were also set around the tower. According to the plot investigation, before thinning, the mean stand density was 1329 stems  $\text{ha}^{-1}$ , and after thinning, it was 849 stems  $\text{ha}^{-1}$  (Table 1). The stand structure characteristics, such as diameter at breast height (DBH), height of trees, and leaf area index (LAI), were also investigated and measured before and after thinning and are listed in Table 1. The LAI was calculated from the TRAC measurements by TRAC-WIN. Canopy openness of the canopy was analyzed from the digital hemispherical photographs by a Sidelook and Gap Light Analyzer (GLA).

### Observation and instrumentation

To investigate the effects of thinning, an eddy covariance (EC) flux observation system was installed at the QYZ site in 2008. After four years of observations, the thinning treatment was conducted in the region encompassing the footprint area of the flux observation. The EC measurement system was installed on the tower at a height of 18.0 m. The EC system included a 3D sonic anemometer (Model CSAT3, Campbell Scientific Inc., Logan, UT, USA) and an open-path  $\text{CO}_2/\text{H}_2\text{O}$  analyzer (Model LI-7500, LI-COR Inc., Lincoln, NE, USA). All signals were collected at a frequency of 10 Hz, and the  $\text{CO}_2$  and  $\text{H}_2\text{O}$  fluxes were calculated and recorded at 30-min intervals by a CR3000 datalogger (Campbell Scientific Inc.).

The environmental factors were observed synchronously. Air temperature ( $T_a$ ), water vapor pressure, and relative humidity were measured via a sensor (Model HMP45C, Vaisala Inc., Helsinki, Finland) in a ventilated solar radiation shield. The soil temperature and soil water content (SWC) were measured at a depth of 5 cm with a temperature sensor (Model 105 T, Campbell Scientific Inc., Logan, USA) and TDR probes (Model CS615-L, Campbell Scientific Inc.), respectively. Radiation was measured via a four-component net radiometer (Model CNR-1, Kipp & Zonen, Delft, ZuidHolland, Netherlands) and a pyranometer (Model CM11, Kipp & Zonen), and the net radiation ( $R_n$ ) was calculated and recorded by the datalogger. Precipitation (PPT) was monitored with a rain gauge (Model 52203, RM Young Inc., Traverse, MI, USA). The environmental variables were sampled at 1 Hz, and 30-min average data were calculated and recorded by a CR1000 datalogger (Campbell Scientific, Inc.).

### Flux data processing

To ensure the reliability and consistency of flux data across China, the ChinaFLUX union has developed a series of standard methods for processing data<sup>43</sup>. Accordingly, in this study, the flux data were processed according to ChinaFLUX standard data processing methods<sup>44</sup>. The raw data were corrected by axis rotation to eliminate the possible influences of local terrain or instrument tilt. The Webb Pearman and Leuning correction (WPL correction)<sup>45</sup> was used to eliminate disturbances introduced by water vapor and temperature. Spurious data caused by system failures or rainfall were removed when the value exceeded the given thresholds for different variables (e.g., for 30-min  $\text{CO}_2$  flux, the thresholds ranged from  $-3 \text{ mg CO}_2 \text{ m}^{-2} \text{ s}^{-1}$  to  $3 \text{ mg CO}_2 \text{ m}^{-2} \text{ s}^{-1}$ ) and then when the anomalous data exceeded the mean  $\pm 3\text{SD}$ . The storage fluxes were subsequently assessed and

	Stand density (stems $\text{ha}^{-1}$ )	Canopy openness (%)	Leaf area index (LAI)	DBH (cm)	Height (m)	Volume ( $\text{m}^3 \text{ha}^{-1}$ )
Pre-thinning	1329	$38.51 \pm 2.16$	$2.94 \pm 0.22$	$15.76 \pm 5.39$	$13.40 \pm 2.46$	$18.70 \pm 2.16$
Post-thinning	849	$44.96 \pm 1.36$	$2.27 \pm 0.08$	$17.18 \pm 5.53$	$13.94 \pm 2.42$	$15.09 \pm 2.21$

**Table 1.** Stand structure characteristics for pre- and post-thinning. The values are the means  $\pm$  SDs.

added to the flux values. To avoid possible underestimation of the fluxes under poor turbulent mixing conditions at night, nighttime (solar elevation angle  $< 0$ ) data were excluded when the friction velocity ( $u^*$ ) was lower than the threshold calculated according to the method described by Reichstein et al.<sup>46</sup>. For the years 2009 to 2014, the average  $u^*$  threshold was  $0.18 \text{ m s}^{-1}$ .

After the anomalous data were excluded, data gaps were generated. Data gaps were filled via the mean diurnal variation method and linear and nonlinear methods<sup>47</sup>. The observed daytime  $\text{CO}_2$  flux is the net ecosystem exchange (NEE), whose absolute value equals the net ecosystem productivity (NEP) but has the opposite sign ( $\text{NEP} = -\text{NEE}$ ), and the nighttime  $\text{CO}_2$  flux equals the ecosystem respiration (Re), which can be extrapolated to the daytime using the Lloyd-Taylor equation to obtain the daytime Re. The GPP was subsequently calculated according to the equation  $\text{GPP} = \text{NEP} + \text{Re}$ . Further detailed information about the flux data correction and calculation can be found in previous relevant studies<sup>48,49</sup>.

### Data analysis

The carbon fluxes and corresponding climatic factors, including Rn, Ta, SWC and VPD were analyzed. To determine the optimum environment for ecosystem GPP, the data before thinning and after thinning were analyzed, respectively. The data were then binned according to each key environmental factor to detect the maximum GPP and the optimum environment. For example, to detect the optimum Rn for GPP, the data were binned into 18 groups, from low to high Rn, and the corresponding average GPP and Rn in each group were obtained. Then, the maximum GPP under the optimum Rn was detected. To determine the optimum environment configuration, the data were subsequently analyzed. For example, to detect the optimum Ta and VPD under certain Rn conditions, the data were first binned according to Rn and then according to Ta and VPD, respectively. The data corrections, calculations, statistical tests, and visualizations were conducted with MATLAB R2023a software (MathWorks Inc., Natick, MA, USA), PyCharm Professional 2023.1 (JetBrains s.r.o., Prague, Czech Republic) and Origin2021 software (Origin Lab Corporation, Northampton, MA, USA).

## Results and discussion

### The theoretical optimum values of key environmental factors before and after thinning

Light, temperature, and water are essential natural resources for photosynthesis. A favorable environment would promote photosynthesis and increase GPP<sup>50–52</sup>. Theoretically, GPP would respond to each environmental factor with an “increase-peak-decrease” pattern<sup>53</sup>. That is, there would be a theoretical optimum value of each environmental factor for GPP. Thus, the responses of the GPP of this subtropical forest to each environmental factor, including Rn, Ta, VPD and SWC, were analyzed before and after thinning (Fig. 1). The results indicated that, except for SWC, the responses of GPP to Rn, Ta, and VPD followed the “increase-peak-decrease” pattern, as expected, which indicated the existence of an optimum value for GPP. Among them, the GPP was highest when Rn reached the optimum value (Fig. 1a and b), indicating the importance of Rn in this subtropical forest<sup>54,55</sup>. In addition, this result indicates this subtropical forest has carbon sink potential to be further explored, as Rn dominated the GPP without other environmental limitations.

The optimum value of each environmental factor for GPP increased after thinning (Fig. 1a–f). The optimum Rn ( $Rn_{\text{opt}}$ ) increased from  $657.18 \text{ J m}^{-2} \text{ s}^{-1}$  to  $719.33 \text{ J m}^{-2} \text{ s}^{-1}$ , the optimum Ta ( $Ta_{\text{opt}}$ ) increased from  $29.66 \text{ }^\circ\text{C}$  to  $30.35 \text{ }^\circ\text{C}$ , and the optimum VPD ( $VPD_{\text{opt}}$ ) increased from  $1.16 \text{ kPa}$  to  $1.25 \text{ kPa}$ . These changes could be attributed to the redistribution of environmental resources and the changing vertical pattern<sup>56</sup>. According to previous studies, light transmittance increased after thinning, and understory light conditions improved because of the openness of the canopy<sup>34</sup>. Consequently, a decrease in canopy closure and improved ventilation may lead to thinned forests being light- and temperature-saturated under conditions of higher Rn and  $Ta$ <sup>38</sup>. Similarly, higher optimum Rn and Ta values were detected in the thinned forest in this study. In addition, the removal of trees would decrease competition for soil water, thereby improving soil water availability, as supported by the study of Cheng et al.<sup>42</sup>, which reported increased SWC following thinning at the QYZ station. The better soil water conditions may help mitigate the stomatal closure tendency induced by high VPD, allowing the forest to maintain higher photosynthetic rates under high VPD. This was evidenced by previous studies, which indicated that a properly high VPD tends to act as a pulling force for vegetation and has two edge effects. If the amount of soil water is sufficient, plants tend to open their stomata under proper high VPD and promote GPP. Otherwise, if there is a shortage of soil water, plants tend to close their stomata to prevent excessive water loss and the occurrence of physiological drought<sup>57–59</sup>. Therefore, owing to the likely increase in soil water availability, the higher  $VPD_{\text{opt}}$  after thinning found in this study is theoretically reasonable. We quantified the changes in the optimum values, which could be useful indicators for future forest carbon sink estimation.

Previous studies also indicated that thinning could alleviate the inhibitory effects of high temperature and low humidity on the stomatal conductance of the upper layer of a forest and thus promote photosynthesis in the remaining trees<sup>60,61</sup>. In addition, thinning increased the contributions of middle- and lower-layer leaves as well as understory shrubs to GPP<sup>62</sup>. These changes, accompanied by a decrease in competition for natural resources, may promote the maximum GPP ( $GPP_{\text{max}}$ ) under optimum environmental conditions<sup>39,40,63</sup>. After thinning, the  $GPP_{\text{max}}$  were found increased in this study, and the  $GPP_{\text{max}}$  under  $Rn_{\text{opt}}$  increased from  $0.82 \text{ mg CO}_2 \text{ m}^{-2} \text{ s}^{-1}$  to  $0.91 \text{ mg CO}_2 \text{ m}^{-2} \text{ s}^{-1}$ , the  $GPP_{\text{max}}$  under  $Ta_{\text{opt}}$  increased from  $0.64 \text{ mg CO}_2 \text{ m}^{-2} \text{ s}^{-1}$  to  $0.72 \text{ mg CO}_2 \text{ m}^{-2} \text{ s}^{-1}$ , and the  $GPP_{\text{max}}$  under  $VPD_{\text{opt}}$  increased from  $0.61 \text{ mg CO}_2 \text{ m}^{-2} \text{ s}^{-1}$  to  $0.67 \text{ mg CO}_2 \text{ m}^{-2} \text{ s}^{-1}$ .

The GPP could be maximized, and its theoretical photosynthesis potential could be realized under  $Rn_{\text{opt}}$ ,  $Ta_{\text{opt}}$  and  $VPD_{\text{opt}}$ . However, it is practically impossible for all three factors to reach their individual optima simultaneously because of natural environmental constraints. Thus, we wanted to know the values of other factors when a given factor achieved the optimum value (Table 2). Therefore, we can comprehensively analyze the most suitable environment that can be achieved in the real world. For both pre- and post-thinning, Ta was closest to  $Ta_{\text{opt}}$  under  $Rn_{\text{opt}}$ . However, the VPD was higher under  $Rn_{\text{opt}}$ . Consequently, under  $Rn_{\text{opt}}$  the coefficients

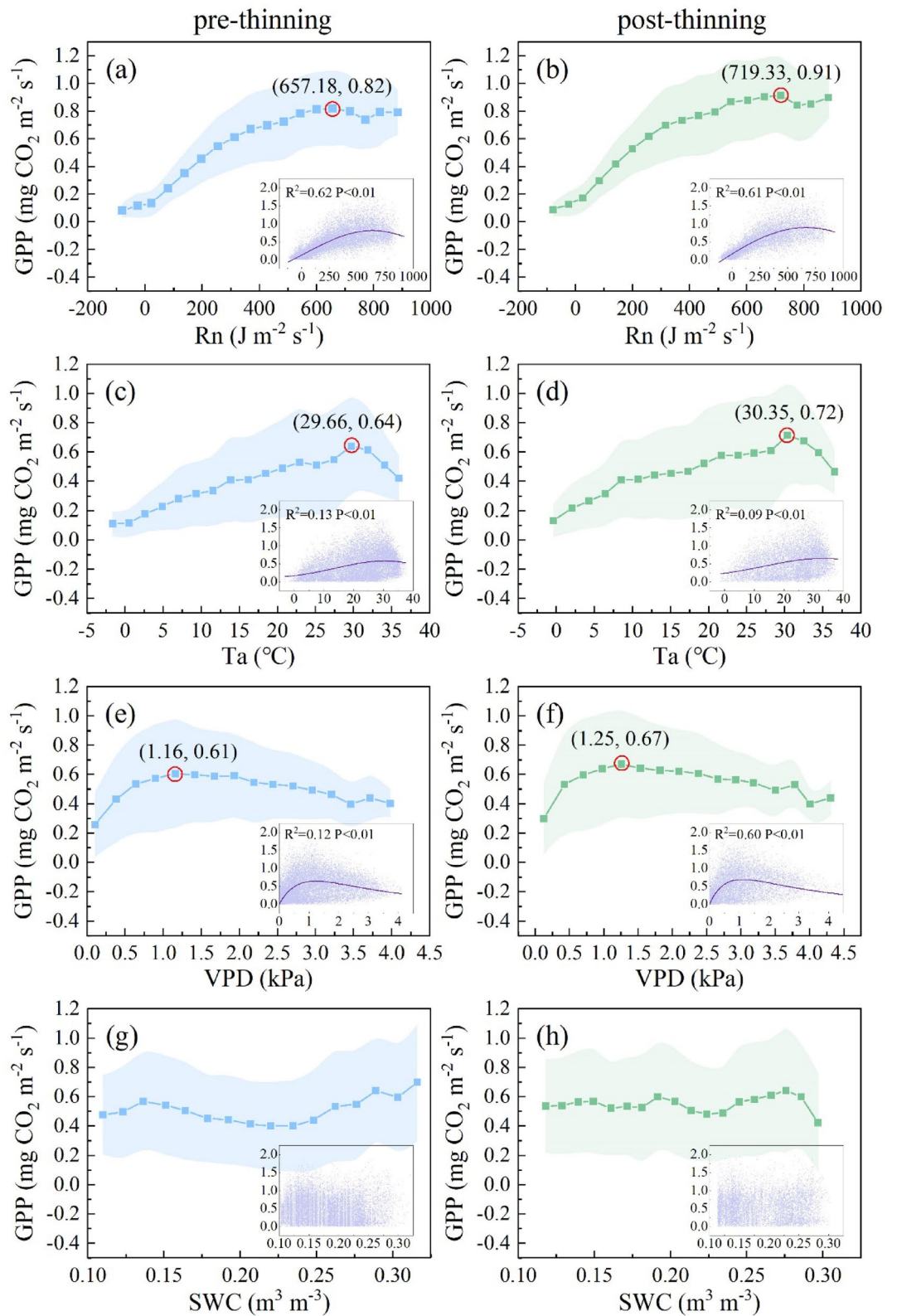


**Fig. 1.** Responses of gross primary productivity (GPP) to environmental factors (net radiation (Rn), air temperature (Ta), vapor pressure deficit (VPD), and soil water content (SWC) at 5 cm depth) before and after thinning. The shadow regions represent the standard deviation. The red circles mark the maximum value points, and (x, y) indicate the optimal values of the environmental variables (optimal Rn ( $Rn_{opt}$ ), optimal Ta ( $Ta_{opt}$ ), and optimal VPD ( $VPD_{opt}$ )) and the corresponding maximum photosynthetic capacity ( $GPP_{max}$ ).

Thinning treatment	Item	Rn ( $\text{J m}^{-2} \text{s}^{-1}$ )	Ta ( $^{\circ}\text{C}$ )	VPD (kPa)	SWC ( $\text{m}^3 \text{m}^{-3}$ )	GPP <sub>max</sub> ( $\text{mg CO}_2 \text{m}^{-2} \text{s}^{-1}$ )
pre-thinning	Rn <sub>opt</sub>	<b>657.18 ± 17.01</b>	28.85 ± 5.13	1.82 ± 0.71	0.17 ± 0.04	0.82 ± 0.27
	Ta <sub>opt</sub>	399.53 ± 230.61	<b>29.66 ± 0.65</b>	1.52 ± 0.50	0.17 ± 0.05	0.64 ± 0.33
	VPD <sub>opt</sub>	334.10 ± 235.60	25.10 ± 4.16	<b>1.16 ± 0.07</b>	0.17 ± 0.04	0.61 ± 0.37
post-thinning	Rn <sub>opt</sub>	<b>719.33 ± 17.53</b>	30.67 ± 3.58	1.95 ± 0.66	0.19 ± 0.05	0.91 ± 0.27
	Ta <sub>opt</sub>	427.29 ± 230.68	<b>30.35 ± 0.64</b>	1.55 ± 0.48	0.19 ± 0.05	0.72 ± 0.35
	VPD <sub>opt</sub>	356.22 ± 234.28	25.53 ± 5.02	<b>1.25 ± 0.08</b>	0.18 ± 0.05	0.67 ± 0.37

**Table 2.** Average values of each environmental factor (net radiation (Rn), air temperature (Ta), vapor pressure deficit (VPD), soil water content (SWC) at 5 cm depth) and maximum photosynthetic capacity (GPP<sub>max</sub>) under the optimum value of the given environmental factor (Rn<sub>opt</sub>, Ta<sub>opt</sub>, and VPD<sub>opt</sub>), which are marked in bold for both pre- and post-thinning.

of favorable light and temperature conditions would promote GPP<sup>64</sup>, but high VPD may depress GPP, as trees tend to close their stomata to prevent damage from physiological water deficiency<sup>65,66</sup>. Under Ta<sub>opt</sub>, Rn was obviously lower than Rn<sub>opt</sub>, and VPD was higher than VPD<sub>opt</sub>. Thus, in this case, Rn could not satisfy the light requirements of the forest, VPD depressed GPP, and the corresponding GPP<sub>max</sub> was lower than GPP<sub>max</sub> under Rn<sub>opt</sub>. Under VPD<sub>opt</sub>, Rn and Ta were both lower than the optimum values, thus leading to the lowest GPP<sub>max</sub> among the three cases (i.e., Rn<sub>opt</sub>, Ta<sub>opt</sub>, and VPD<sub>opt</sub>).

According to the results in Table 2, when a single environmental factor reached its theoretical optimum, the other factors often deviated substantially from their respective optimum. Consequently, the GPP observed under such single-factor optimum conditions failed to represent the maximum photosynthetic capacity of the ecosystem<sup>20</sup>. However, we found that the GPP<sub>max</sub> increased with the increasing number of factors approaching their optimal ranges. In this subtropical forest, both before and after thinning, this occurred under Rn<sub>opt</sub>, when the GPP<sub>max</sub> was higher than that under Ta<sub>opt</sub> and VPD<sub>opt</sub>.

### The optimum Ta combining with Rn and the thinning effects

Since it is difficult for Rn, Ta, and VPD to reach their optimal values simultaneously under natural conditions, we explored the combination of environmental factors that can maximize GPP under actual environmental conditions, that is, the optimal photosynthetic environment. According to the R<sup>2</sup> values between GPP and the environmental factors, the correlation between GPP and Rn was significantly higher than that between GPP and the other environmental factors (Fig. 1). To further clarify the optimal photosynthetic environment configuration, we analyzed the response of GPP to Ta and VPD under different Rn conditions. The GPP did not change obviously with increasing SWC, which may be attributed to the influence of SWC being primarily manifested under drought conditions as a limiting factor, rather than exerting a direct promoting effect on GPP<sup>67,68</sup>. The underlying mechanisms through which SWC influences forest ecosystems differ from those of other environmental factors, and its response pattern may not follow the “increase-peak-decrease” pattern<sup>68</sup>. Therefore, the effects of SWC are not further discussed in this study.

The response of GPP to Ta has been widely reported, with a consensus on the existence of an optimum Ta under natural conditions<sup>15,16</sup>. However, when the analyses were conducted according to different Rn classes on the basis of the large dataset, interesting regulations emerged (Fig. 2). It could be found that when Rn was lower than  $180 \text{ J m}^{-2} \text{ s}^{-1}$ , the GPP did not exhibit an obvious response to elevated Ta due to insufficient light. This is reasonable, as the photosynthetic apparatus cannot capture sufficient photons; thus, the energy cannot sustain stronger photosynthesis<sup>10,69</sup>. When Rn was higher than  $180 \text{ J m}^{-2} \text{ s}^{-1}$ , the effects of Ta began to emerge. Ta<sub>opt</sub> increased with increasing Rn both before and after thinning and approached the optimum values detected in Fig. 1 (Fig. 2m). Before thinning, Ta<sub>opt</sub> sharply increased in the Rn class of  $480 \leq \text{Rn} < 630 \text{ J m}^{-2} \text{ s}^{-1}$ , from  $20.70 \text{ }^{\circ}\text{C}$  in the previous Rn class ( $330 \leq \text{Rn} < 480 \text{ J m}^{-2} \text{ s}^{-1}$ ) to  $26.35 \text{ }^{\circ}\text{C}$  (Fig. 2d and e). While after thinning, Ta<sub>opt</sub> sharply increased to  $26.54 \text{ }^{\circ}\text{C}$  in the Rn class of  $330 \leq \text{Rn} < 480 \text{ J m}^{-2} \text{ s}^{-1}$  (Fig. 2j), which occurred earlier than pre-thinning. The response divergence could be more directly observed in Fig. 2m, indicating that thinning enabled the forest to maintain higher GPP even under lower Rn conditions. This indicated an improvement in light use efficiency following thinning, as the vegetation exhibited enhanced responses to Ta without being constrained by light limitation. This finding is consistent with the findings reported by previous studies, which reported that plants could use weak light more efficiently after thinning<sup>70,71</sup>. As Rn increased, it approached the respective optima identified in Fig. 1c and d, which were  $29.66 \text{ }^{\circ}\text{C}$  and  $30.35 \text{ }^{\circ}\text{C}$  before and after thinning, respectively. Thus, the GPP<sub>max</sub> increased in the higher Rn classes, and the values were always higher for post-thinning than pre-thinning (Fig. 2n), indicating that thinning enhanced the photosynthetic capacity of this coniferous forest.

In the step by step analysis progress for detecting the optimum photosynthetic environment, we could find that in the Rn class of  $\text{Rn} > 630 \text{ J m}^{-2} \text{ s}^{-1}$ , when Ta reached Ta<sub>opt</sub>, the corresponding GPP<sub>max</sub> (Fig. 2f and l) exceeded the values observed under Rn<sub>opt</sub> alone (Fig. 1a and b). In detail, for pre-thinning, when Ta achieved Ta<sub>opt</sub> of  $27.03 \text{ }^{\circ}\text{C}$  under the circumstance of  $\text{Rn} > 630 \text{ J m}^{-2} \text{ s}^{-1}$ , the GPP<sub>max</sub> was  $0.89 \text{ mg CO}_2 \text{ m}^{-2} \text{ s}^{-1}$  (Fig. 2f), which was higher than the GPP<sub>max</sub> of  $0.82 \text{ mg CO}_2 \text{ m}^{-2} \text{ s}^{-1}$  found under Rn<sub>opt</sub> (Fig. 1a). For post-thinning, the corresponding Ta<sub>opt</sub> was  $27.30 \text{ }^{\circ}\text{C}$ , and the GPP<sub>max</sub> was  $1.01 \text{ mg CO}_2 \text{ m}^{-2} \text{ s}^{-1}$  (Fig. 2l), which was higher than the GPP<sub>max</sub> of  $0.91 \text{ mg CO}_2 \text{ m}^{-2} \text{ s}^{-1}$  under Rn<sub>opt</sub> (Fig. 1b). This finding indicates that identifying the “optimal photosynthetic environment configuration” (a combination of multiple factors that cooccur under natural conditions and maximize GPP) is more practically significant than focusing solely on theoretical single-factor

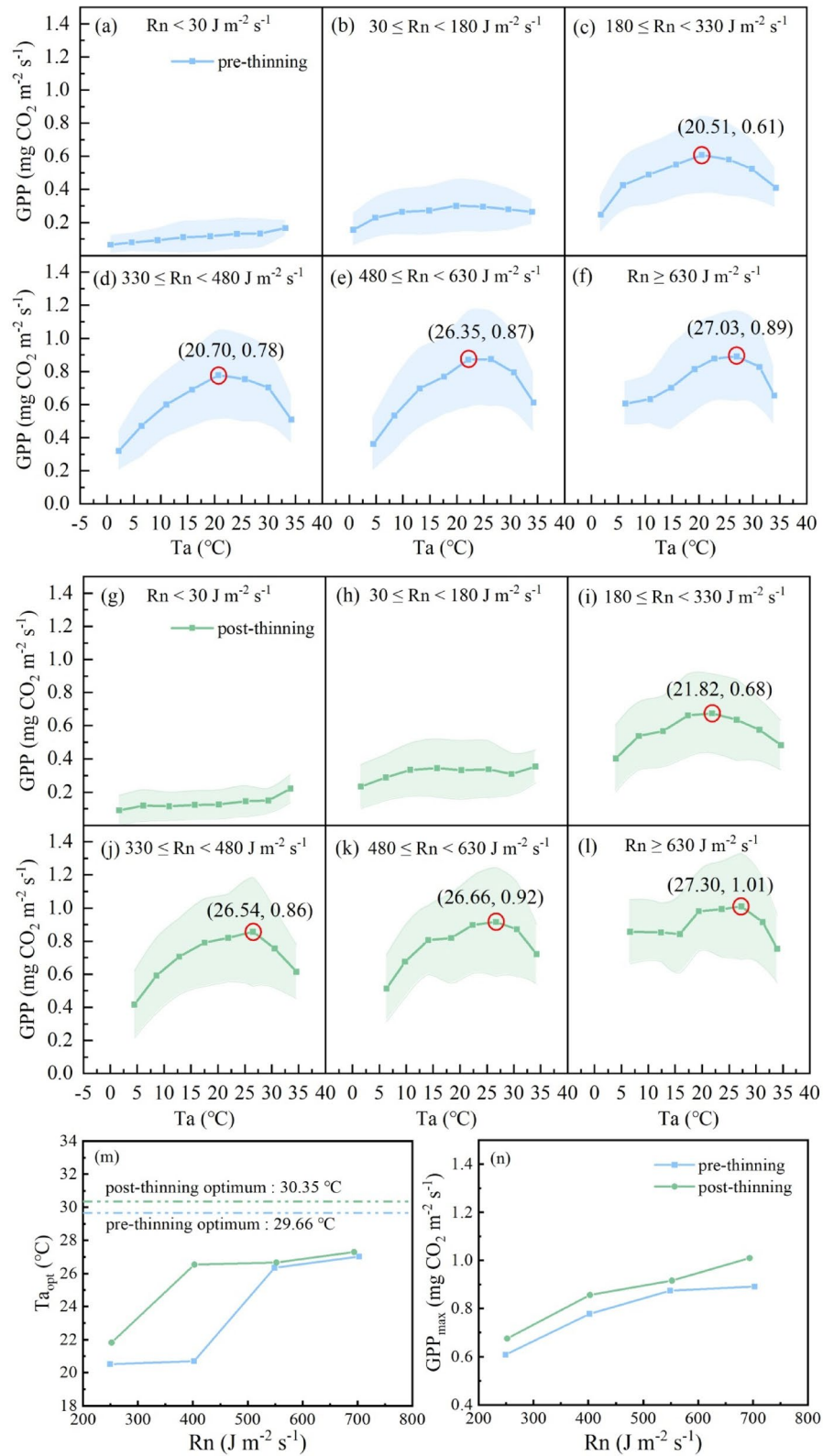


**Fig. 2.** Responses of gross primary productivity (GPP) to air temperature (Ta) in different net radiation (Rn) classes before and after thinning. The shaded areas represent the standard deviation. The maximum values in each Rn class are marked with red circles, and the point (x, y) indicates the optimal Ta (Ta<sub>opt</sub>) and maximum photosynthetic capacity (GPP<sub>max</sub>) in different Rn classes. The trends of Ta<sub>opt</sub> and GPP<sub>max</sub> along with differing Rn classes are shown in panels (m) and (n).

optima. Notably, after thinning, the  $GPP_{max}$  under this “high radiation and optimal temperature” configuration was substantially higher than that before thinning. These findings indicate that thinning, by altering the canopy and vertical structure of the forest and affecting the microclimate, likely enhances natural resource utilization efficiency, thereby further improving the photosynthetic potential of the forest under optimal environmental configurations. We first confirmed the predominant role of Rn in determining the optimum photosynthetic environment, as shown in Fig. 1. To date, we have found a better environment configuration for GPP based on the single environmental optimum shown in Fig. 1. Furthermore, the combination of VPD and Rn for better environment configuration was studied.

### The optimum VPD combining with Rn and the thinning effects

The responses of GPP to VPD under different Rn conditions were analyzed both before and after thinning (Fig. 3). When Rn was lower than  $180 \text{ J m}^{-2} \text{ s}^{-1}$ , the GPP remained low and did not change with increasing VPD, indicating the dominant control effects of Rn on ecosystem photosynthesis<sup>54</sup>. In the middle and high Rn classes, the influence of VPD on GPP became evident. The GPP increased with VPD until  $VPD_{opt}$  and then decreased, following the expected pattern, as previously indicated by the existence of a response peak<sup>65</sup>. As Rn increased,  $VPD_{opt}$  increased both before and after thinning, approaching the theoretical single-factor optimum as previously identified (Fig. 3m). Consequently, the  $GPP_{max}$  increased in the higher Rn classes (Fig. 3n). It could be found that  $Ta_{opt}$  and  $VPD_{opt}$  simultaneously got to their respective optimal values in the higher Rn classes, which supported the predominant role of Rn in regulating GPP (Figs. 2m and 3m).

The post-thinning  $VPD_{opt}$  and corresponding  $GPP_{max}$  values were always higher than those before thinning across all Rn classes (Fig. 3n). This finding indicates that, to some extent, thinning alleviated the adverse effects of high VPD-induced atmospheric drought stress<sup>23,72</sup>. In combination with reduced soil water competition due to tree removal<sup>61,73</sup>, a moderately high VPD likely contributed to higher GPP. This is reasonable, as relatively high VPD under sufficient soil water availability promotes stomatal opening; therefore, more  $\text{CO}_2$  enters the photosynthetic apparatus and improves light and heat use efficiency, ultimately increasing GPP<sup>57,74,75</sup>.

For the optimum environment configuration, before thinning, we found that in the class of  $Rn > 630 \text{ J m}^{-2} \text{ s}^{-1}$ , when the  $VPD_{opt}$  was 0.96 kPa, the corresponding  $GPP_{max}$  could reach  $0.98 \text{ mg CO}_2 \text{ m}^{-2} \text{ s}^{-1}$  (Fig. 3f), which was higher than the  $GPP_{max}$  found under sole  $Rn_{opt}$  and the previously mentioned  $Ta_{opt}$  under  $Rn > 630 \text{ J m}^{-2} \text{ s}^{-1}$  (Figs. 1a and 2f). Thus, this case might refer to the circumstances under which the optimum environment configuration occurred. Similarly, for post-thinning, the corresponding  $VPD_{opt}$  was 1.10 kPa, and the  $GPP_{max}$  was found to have the highest value of  $1.11 \text{ mg CO}_2 \text{ m}^{-2} \text{ s}^{-1}$  (Fig. 3l), which was higher than that under sole  $Rn_{opt}$  and the previously mentioned  $Ta_{opt}$  under  $Rn > 630 \text{ J m}^{-2} \text{ s}^{-1}$  reported in Figs. 1b and 2l.

### The optimal photosynthetic environment and the changes induced by thinning

The optimum photosynthetic environment for pre-thinning and post-thinning could be identified according to the previous analyses when  $GPP_{max}$  reached the maximum value. The averages of other factors were subsequently calculated to provide accurate quantified indicators for this subtropical forest. According to the results in Table 3, the optimum photosynthetic environment that can be achieved in the real world for pre-thinning was  $Rn = 692.85 \text{ J m}^{-2} \text{ s}^{-1}$ ,  $Ta = 23.43 \text{ }^\circ\text{C}$ ,  $VPD = 0.96 \text{ kPa}$  and  $SWC = 0.20 \text{ m}^3 \text{ m}^{-3}$ , with a corresponding  $GPP_{max}$  of  $0.98 \text{ mg CO}_2 \text{ m}^{-2} \text{ s}^{-1}$ . After thinning, the optimum photosynthetic environment changed to  $Rn = 693.92 \text{ J m}^{-2} \text{ s}^{-1}$ ,  $Ta = 26.70 \text{ }^\circ\text{C}$ ,  $VPD = 1.10 \text{ kPa}$  and  $SWC = 0.21 \text{ m}^3 \text{ m}^{-3}$ , with a corresponding  $GPP_{max}$  of  $1.11 \text{ mg CO}_2 \text{ m}^{-2} \text{ s}^{-1}$ .

According to the results, the optimum photosynthetic environment that can actually be achieved in reality does not completely align with the optimal values of each single environmental factor (Tables 2 and 3). Generally, the values of each environmental factor in the real optimal photosynthetic environment are generally lower than their respective single-factor optimal values, indicating that the optimal photosynthetic environment is by no means a simple combination of the optimal values of each environmental factor but rather a complex combination regulated by mutual influences<sup>13,21</sup>.

The values of each environmental factor in the optimum photosynthetic environment after thinning were all higher than those before thinning, indicating that thinning could improve the resource utilization capacity of the initially overly dense forest ecosystem<sup>39,40,63,76</sup>; thus, the  $GPP_{max}$  was greater after thinning (Fig. 3). This was consistent with the results of the single-factor optimal values, which proved that thinning improved the microclimate environment, enhanced the resource utilization capacity of vegetation, and thereby increased the photosynthetic capacity of the forest.

## Conclusions

The photosynthetic capacity of vegetation is greatly determined by environmental conditions, and the extent to which it can achieve maximum photosynthesis depends on how favorable those conditions are. However, under natural conditions, the specific optimal values of each environmental factor for GPP rarely occur simultaneously. Therefore, based on clarification of the optimal values of each single factor, this study further conducted a comprehensive analysis to identify the optimal photosynthetic environment configuration (including multiple environmental factors) that this subtropical planted forest ecosystem can achieve under natural conditions before and after thinning. Before thinning, the optimum photosynthetic environment configuration was  $Rn = 692.85 \text{ J m}^{-2} \text{ s}^{-1}$ ,  $Ta = 23.43 \text{ }^\circ\text{C}$ ,  $VPD = 0.96 \text{ kPa}$  and soil water content ( $SWC$ ) =  $0.20 \text{ m}^3 \text{ m}^{-3}$ . After thinning, the optimum configuration changed to  $Rn = 693.92 \text{ J m}^{-2} \text{ s}^{-1}$ ,  $Ta = 26.70 \text{ }^\circ\text{C}$ ,  $VPD = 1.10 \text{ kPa}$  and  $SWC = 0.21 \text{ m}^3 \text{ m}^{-3}$ . Correspondingly, the  $GPP_{max}$  increased from  $0.98$  to  $1.11 \text{ mg CO}_2 \text{ m}^{-2} \text{ s}^{-1}$  after thinning. The optimum values of key environmental factors for ecosystem photosynthesis all elevated after thinning. This might be one of the reasons why thinning increases the carbon sequestration capacity of this subtropical plantation. In addition, for both pre- and post-thinning, the  $GPP_{max}$  under the optimal photosynthetic environment configuration was

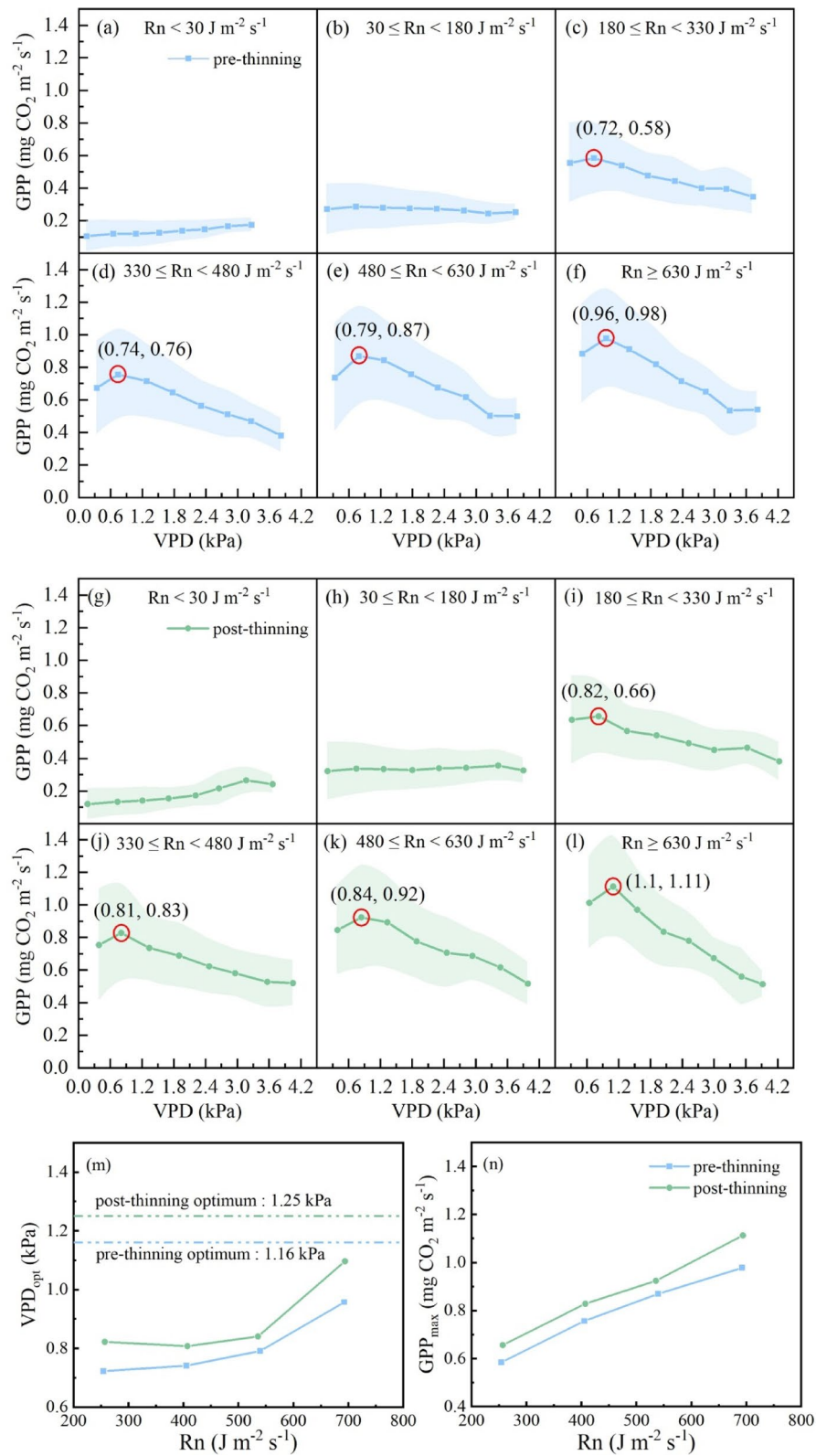


**Fig. 3.** Responses of gross primary productivity (GPP) to vapor pressure deficit (VPD) in different net radiation (Rn) classes before and after thinning. The shaded areas represent the standard deviation. The maximum values in each Rn class are marked with red circles, and the point (x, y) indicates the optimal VPD ( $VPD_{opt}$ ) and maximum photosynthetic capacity ( $GPP_{max}$ ) in different Rn classes. The trends of  $VPD_{opt}$  and  $GPP_{max}$  along with differing Rn classes are shown in panels (m) and (n).

Thinning treatment	Rn (J m <sup>-2</sup> s <sup>-1</sup> )	Ta (°C)	VPD (kPa)	SWC (m <sup>3</sup> m <sup>-3</sup> )	GPP <sub>max</sub> (mg CO <sub>2</sub> m <sup>-2</sup> s <sup>-1</sup> )
pre-thinning	692.85 ± 51.38	23.43 ± 5.71	0.96 ± 0.14	0.20 ± 0.04	0.98 ± 0.30
post-thinning	693.92 ± 53.96	26.70 ± 4.16	1.10 ± 0.13	0.21 ± 0.05	1.11 ± 0.31

**Table 3.** Comparisons of the optimal photosynthetic environment (net radiation (Rn), air temperature (Ta), vapor pressure deficit (VPD), soil water content (SWC) at 5 cm depth) and maximum photosynthetic capacity (GPP<sub>max</sub>) before and after thinning.

always higher than the GPP<sub>max</sub> when a single factor reached its optimum. These results manifested that thinning elevated the optimum environmental conditions and ecosystem photosynthetic capacity, and the optimum environment configuration that realistically occurs in the natural world is a more important indicator of GPP<sub>max</sub> compared to the single-factor optimum, which should be taken into more careful consideration when assessing the impact of climate change on the carbon sink function of terrestrial ecosystems.

### Data availability

Data of this study are available from the corresponding authors upon reasonable request.

Received: 20 July 2025; Accepted: 1 January 2026

Published online: 08 January 2026

### References

- Keenan, T. F. et al. Recent pause in the growth rate of atmospheric CO<sub>2</sub> due to enhanced terrestrial carbon uptake. *Nat. Commun.* **7**, 13428. <https://doi.org/10.1038/ncomms13428> (2016).
- Fettig, C. J. et al. Changing climates, changing forests: A Western North American perspective. *J. For.* **111**, 214–228. <https://doi.org/10.5849/jof.12-085> (2013).
- Pau, S., Detto, M., Kim, Y. & Still, C. J. Tropical forest temperature thresholds for gross primary productivity. *Ecosphere* **9**, e02311. <https://doi.org/10.1002/ecs2.2311> (2018).
- Liu, X. et al. Compound droughts slow down the greening of the Earth. *Global Change Biol.* **29**, 3072–3084. <https://doi.org/10.1111/gcb.16657> (2023).
- Vicente-Serrano, S. M., Quiring, S. M., Pena-Gallardo, M., Yuan, S. & Dominguez-Castro, F. A review of environmental droughts: increased risk under global warming?. *Earth Sci. Rev.* **201**, 102953. <https://doi.org/10.1016/j.earscirev.2019.102953> (2020).
- Yang, B., Wen, X. & Sun, X. Seasonal variations in depth of water uptake for a subtropical coniferous plantation subjected to drought in an East Asian monsoon region. *Agric. Meteorol.* **201**, 218–228. <https://doi.org/10.1016/j.agrformet.2014.11.020> (2015).
- Bussotti, F., Pollastrini, M., Holland, V. & Brueggemann, W. Functional traits and adaptive capacity of European forests to climate change. *Environ. Exp. Bot.* **111**, 91–113. <https://doi.org/10.1016/j.envexpbot.2014.11.006> (2015).
- Green, J. K., Berry, J., Ciaia, P., Zhang, Y. & Gentine, P. Amazon rainforest photosynthesis increases in response to atmospheric dryness. *Sci. Adv.* **6**, eabb7232. <https://doi.org/10.1126/sciadv.abb7232> (2020).
- Miller, B. D., Carter, K. R., Reed, S. C., Wood, T. E. & Cavaleri, M. A. Only sun-lit leaves of the uppermost canopy exceed both air temperature and photosynthetic thermal Optima in a wet tropical forest. *Agric. Meteorol.* **301**, 108347. <https://doi.org/10.1016/j.agrformet.2021.108347> (2021).
- de Oliveira, I. V., da Costa, K. C. P., da Rocha Nina Junior, A., de Carvalho, J. C. & de Carvalho Goncalves, J. F. Brazil nut tree increases photosynthetic activity and stem diameter growth after thinning. *Theor. Exp. Plant. Physiol.* **36**, 251–263. <https://doi.org/10.1007/s40626-024-00317-4> (2024).
- Man, R. & Greenway, K. J. Effects of artificial shade on early performance of white Spruce seedlings planted on clearcuts. *New. For.* **41**, 221–233. <https://doi.org/10.1007/s11056-010-9223-y> (2011).
- Gunderson, C. A., O'Hara, K. H., Campion, C. M., Walker, A. V. & Edwards, N. T. Thermal plasticity of photosynthesis: The role of acclimation in forest responses to a warming climate. *Global Change Biol.* **16**, 2272–2286. <https://doi.org/10.1111/j.1365-2486.2009.02090.x> (2010).
- Slot, M., Rifai, S. W., Eze, C. E. & Winter, K. The stomatal response to vapor pressure deficit drives the apparent temperature response of photosynthesis in tropical forests. *New. Phytol.* **244**, 1238–1249. <https://doi.org/10.1111/nph.19806> (2024).
- Fujita, S., Noguchi, K. & Tange, T. Different waterlogging depths affect Spatial distribution of fine root growth for *Pinus thunbergii* seedlings. *Front. Plant. Sci.* **12**, 614764. <https://doi.org/10.3389/fpls.2021.614764> (2021).
- Huang, M. et al. Air temperature Optima of vegetation productivity across global biomes. *Nat. Ecol. Evol.* **3**, 772–779. <https://doi.org/10.1038/s41559-019-0838-x> (2019).
- Kumarathunge, D. P. et al. Photosynthetic temperature responses in leaves and canopies: Why temperature Optima May disagree at different scales. *Tree Physiol.* **44**, tpa135. <https://doi.org/10.1093/treephys/tpae135> (2024).
- Marchin, R. M., Broadhead, A. A., Bostic, L. E., Dunn, R. R. & Hoffmann, W. A. Stomatal acclimation to vapour pressure deficit doubles transpiration of small tree seedlings with warming. *Plant. Cell. Environ.* **39**, 2221–2234. <https://doi.org/10.1111/pce.12790> (2016).
- Sharp, E. D., Sullivan, P. F., Steltzer, H., Csank, A. Z. & Welker, J. M. Complex carbon cycle responses to multi-level warming and supplemental summer rain in the high Arctic. *Global Change Biol.* **19**, 1780–1792. <https://doi.org/10.1111/gcb.12149> (2013).
- Xu, X. J. et al. Eddy covariance analysis of the implications of drought on the carbon fluxes of Moso bamboo forest in southeastern China. *Trees-Struct Funct.* **30**, 1807–1820. <https://doi.org/10.1007/s00468-016-1414-5> (2016).
- Zhang, T. et al. Analysis of the optimal photosynthetic environment for an alpine meadow ecosystem. *Agric. Meteorol.* **341**, 109651. <https://doi.org/10.1016/j.agrformet.2023.109651> (2023).
- Eze, C. E., Winter, K. & Slot, M. Vapor-pressure-deficit-controlled temperature response of photosynthesis in tropical trees. *Photosynthetica* **62**, 318–325. <https://doi.org/10.32615/ps.2024.034> (2024).
- Xu, M. et al. The responses of photosynthetic light response parameters to temperature among different seasons in a coniferous plantation of subtropical China. *Ecol. Indic.* **145**, 109595. <https://doi.org/10.1016/j.ecolind.2022.109595> (2022).
- Zhang, L. et al. Seasonal variations of ecosystem apparent quantum yield (α) and maximum photosynthesis rate (P<sub>max</sub>) of different forest ecosystems in China. *Agric. Meteorol.* **137**, 176–187. <https://doi.org/10.1016/j.agrformet.2006.02.006> (2006).
- Niu, S. et al. Thermal optimality of net ecosystem exchange of carbon dioxide and underlying mechanisms. *New. Phytol.* **194**, 775–783. <https://doi.org/10.1111/j.1469-8137.2012.04095.x> (2012).

25. IPCC. *Climate Change 2021 – The Physical Science Basis: Working Group I Contribution To the Sixth Assessment Report of the Intergovernmental Panel on Climate Change* (Cambridge University Press, 2023).
26. Marini, L. et al. Climate drivers of bark beetle outbreak dynamics in Norway Spruce forests. *Ecography* **40**, 1426–1435. <https://doi.org/10.1111/ecog.02769> (2017).
27. Seliger, A., Ammer, C., Kreft, H. & Zerbe, S. Diversification of coniferous monocultures in the last 30 years and implications for forest restoration: A case study from temperate lower montane forests in central Europe. *Eur. J. Res.* **142**, 1353–1368. <https://doi.org/10.1007/s10342-023-01595-4> (2023).
28. Cheng, C. et al. Thinning effect on understory community and photosynthetic characteristics in a subtropical *Pinus massoniana* plantation. *Can. J. Res.* **47**, 1104–1115. <https://doi.org/10.1139/cjfr-2017-0082> (2017).
29. Ji, L., Wang, Z., Wang, X. & An, L. Forest insect pest management and forest management in china: An overview. *Environ. Manage.* **48**, 1107–1121. <https://doi.org/10.1007/s00267-011-9697-1> (2011).
30. Moreau, G. et al. Opportunities and limitations of thinning to increase resistance and resilience of trees and forests to global change. *Forestry* **95**, 595–615. <https://doi.org/10.1093/forestry/cpac010> (2022).
31. Zhang, H. et al. Thinning increases forest ecosystem carbon stocks. *Ecol. Manage.* **555**, 121702. <https://doi.org/10.1016/j.foreco.2024.121702> (2024).
32. Li, Y., Hong, S., Fang, S. & Cui, G. Thinning promotes litter decomposition and nutrient release in Poplar plantations via altering the microclimate and understory plant diversity. *Ann. Res.* **66**, 3–18. <https://doi.org/10.15287/afr.2023.2231> (2023).
33. Rambo, T. R. & North, M. P. Canopy microclimate response to pattern and density of thinning in a Sierra Nevada forest. *Ecol. Manag.* **257**, 435–442. <https://doi.org/10.1016/j.foreco.2008.09.029> (2009).
34. Gauthier, M. M. & Jacobs, D. F. Short-term physiological responses of black walnut (*Juglans Nigra* L.) to plantation thinning. *For. Sci.* **55**, 221–229. <https://doi.org/10.1093/forestscience/55.3.221> (2009).
35. Sankey, T. & Tatum, J. Thinning increases forest resiliency during unprecedented drought. *Sci. Rep.* **12**, 9041. <https://doi.org/10.1038/s41598-022-12982-z> (2022).
36. Vesala, T. et al. Effect of thinning on surface fluxes in a boreal forest. *Global Biogeochem. Cy.* **19**, GB2001. <https://doi.org/10.1029/2004GB002316> (2005).
37. Mazza, G., Amorini, E., Cutini, A. & Manetti, M. C. The influence of thinning on rainfall interception by *Pinus Pinea* L. in mediterranean coastal stands (Castel Fusano-Rome). *Ann. Sci.* **68**, 1323–1332. <https://doi.org/10.1007/s13595-011-0142-7> (2011).
38. Deng, C. et al. Thinning effects on forest evolution in Masson pine (*Pinus massoniana* Lamb.) conversion from pure plantations into mixed forests. *Ecol. Manag.* **477**, 118503. <https://doi.org/10.1016/j.foreco.2020.118503> (2020).
39. Forrester, D. I., Collopy, J. J., Beadle, C. L. & Baker, T. G. Effect of thinning, pruning and nitrogen fertiliser application on light interception and light-use efficiency in a young *Eucalyptus nitens* plantation. *Ecol. Manage.* **288**, 21–30. <https://doi.org/10.1016/j.foreco.2011.11.024> (2013).
40. Martín-Benito, D., Río, D., Heinrich, M., Helle, I. & Cañellas, I. Response of climate-growth relationships and water use efficiency to thinning in a *Pinus Nigra* afforestation. *Ecol. Manag.* **259**, 967–975. <https://doi.org/10.1016/j.foreco.2009.12.001> (2010).
41. Xu, M. J. et al. The Estimation and partitioning of evapotranspiration in a coniferous plantation in subtropical China. *Front. Plant. Sci.* **14**, 1120202. <https://doi.org/10.3389/fpls.2023.1120202> (2023).
42. Cheng, C. P. et al. Effects of thinning on forest soil and stump respiration in a subtropical pine plantation. *Ecol. Manag.* **531**, 120797. <https://doi.org/10.1016/j.foreco.2023.120797> (2023).
43. Yu, G., Fu, Y., Sun, X., Wen, X. & Zhang, L. Recent progress and future directions of ChinaFLUX. *Sci. China Ser. D: Earth Sci.* **49**, 1–23. <https://doi.org/10.1007/s11430-006-8001-3> (2006).
44. Yu, G., Wen, X., Sun, X. & Bertrand Overview of ChinaFLUX and evaluation of its eddy covariance measurement. *Agric. Meteorol.* **137**, 125–137. <https://doi.org/10.1016/j.agrformet.2006.02.011> (2006).
45. Webb, E. K., Pearman, G. I. & Leuning, R. G. Correction of flux measurements for density effects due to heat and water-vapor transfer. *Q. J. R. Meteorol. Soc.* **106**, 85–100. <https://doi.org/10.1002/qj.49710644707> (1980).
46. Reichstein, M., Falge, E., Baldocchi, D., Papale, D. & Valentini, R. On the separation of net ecosystem exchange into assimilation and ecosystem respiration: Review and improved algorithm. *Global Change Biol.* **11**, 1424–1439. <https://doi.org/10.1111/j.1365-2486.2005.001002.x> (2005).
47. Falge, E., Baldocchi, D., Olson, R., Anthoni, P. & Tu, K. Gap filling strategies for defensible annual sums of net ecosystem exchange. *Agric. Meteorol.* **107**, 43–69. [https://doi.org/10.1016/S0168-1923\(00\)00225-2](https://doi.org/10.1016/S0168-1923(00)00225-2) (2001).
48. Xu, M. J. et al. Effects of Climatic factors and ecosystem responses on the inter-annual variability of evapotranspiration in a coniferous plantation in subtropical China. *PLoS One.* **9**, e85593. <https://doi.org/10.1371/journal.pone.0085593> (2014).
49. Xu, M. J. et al. The full annual carbon balance of a subtropical coniferous plantation is highly sensitive to autumn precipitation. *Sci. Rep.* **7**, 10025. <https://doi.org/10.1038/s41598-017-10485-w> (2017).
50. Teskey, R. et al. Responses of tree species to heat waves and extreme heat events. *Plant. Cell. Environ.* **38**, 1699–1712. <https://doi.org/10.1111/pce.12417> (2015).
51. Grossiord, C. et al. Plant responses to rising vapor pressure deficit. *New. Phytol.* **226**, 1550–1566. <https://doi.org/10.1111/nph.16485> (2020).
52. Xia, J. et al. Joint control of terrestrial gross primary productivity by plant phenology and physiology. *Proc. Natl. Acad. Sci. U S A.* **112**, 2788–2793. <https://doi.org/10.1073/pnas.1413090112> (2015).
53. Zhang, T. et al. Soil moisture alters the responses of alpine ecosystem productivity to environmental factors, especially VPD, on the Qinghai-Tibetan plateau. *Sci. Total Environ.* **947**, 174518. <https://doi.org/10.1016/j.scitotenv.2024.174518> (2024).
54. Han, J. et al. Effects of diffuse photosynthetically active radiation on gross primary productivity in a subtropical coniferous plantation vary in different timescales. *Ecol. Indic.* **115**, 106403. <https://doi.org/10.1016/j.ecolind.2020.106403> (2020).
55. Xu, H., Zhang, Z. Q., Chen, J. Q., Zhu, M. X. & Kang, M. C. Cloudiness regulates gross primary productivity of a Poplar plantation under different environmental conditions. *Can. J. Res.* **47**, 648–658. <https://doi.org/10.1139/cjfr-2016-0413> (2017).
56. Prévost, M. & Raymond, P. Effect of gap size, aspect and slope on available light and soil temperature after patch-selection cutting in yellow birch–conifer stands, Quebec, Canada. *Ecol. Manage.* **274**, 210–221. <https://doi.org/10.1016/j.foreco.2012.02.020> (2012).
57. Chen, N. et al. Divergent impacts of atmospheric water demand on gross primary productivity in three typical ecosystems in China. *Agric. Meteorol.* **307**, 108527. <https://doi.org/10.1016/j.agrformet.2021.108527> (2021).
58. Magruder, M., Chhin, S., Palik, B. & Bradford, J. B. Thinning increases climatic resilience of red pine. *Can. J. Res.* **43**, 878–889. <https://doi.org/10.1139/cjfr-2013-0088> (2013).
59. Meijers, E. et al. Canopy cover at the crown-scale best predicts spatial heterogeneity of soil moisture within a temperate Atlantic forest. *Agric. Meteorol.* **363**, 110431. <https://doi.org/10.1016/j.agrformet.2025.110431> (2025).
60. Bachofen, C., D’Oro, P. & Buchmann, N. Light and VPD gradients drive foliar nitrogen partitioning and photosynthesis in the canopy of European Beech and silver Fir. *Oecologia* **192**, 323–339. <https://doi.org/10.1007/s00442-019-04583-x> (2020).
61. Zhang, Z. et al. Forest water-use efficiency: Effects of climate change and management on the coupling of carbon and water processes. *Ecol. Manage.* **534**, 120853. <https://doi.org/10.1016/j.foreco.2023.120853> (2023).
62. dos Santos, V., Modolo, G. S. & Ferreira, M. J. How do silvicultural treatments alter the microclimate in a central Amazon secondary forest? A focus on light changes. *J. Environ. Manag.* **254**, 109816. <https://doi.org/10.1016/j.jenvman.2019.109816> (2020).
63. Kanniah, K. D., Beringer, J. & Hurley, L. Exploring the link between clouds, radiation, and canopy productivity of tropical savannas. *Agric. Meteorol.* **182**, 304–313. <https://doi.org/10.1016/j.agrformet.2013.06.010> (2013).

64. Xu, C. et al. Light more than warming impacts understory tree seedling growth in a temperate deciduous forest. *Ecol. Manage.* **549**, 121496. <https://doi.org/10.1016/j.foreco.2023.121496> (2023).
65. Goodrich, J. P., Campbell, D. I., Clearwater, M. J., Rutledge, S. & Schipper, L. A. High vapor pressure deficit constrains GPP and the light response of NEE at a Southern hemisphere bog. *Agric. Meteorol.* **203**, 54–63. <https://doi.org/10.1016/j.agrformet.2015.01.001> (2015).
66. Xu, M. et al. Specific responses of canopy conductance to environmental factors in a coniferous plantation in subtropical China. *Ecol. Indic.* **131**, 108168. <https://doi.org/10.1016/j.ecolind.2021.108168> (2021).
67. Bachofen, C. et al. Stand structure of central European forests matters more than climate for transpiration sensitivity to VPD. *J. Appl. Ecol.* **60**, 886–897. <https://doi.org/10.1111/1365-2664.14383> (2023).
68. Novick, K. A. et al. The increasing importance of atmospheric demand for ecosystem water and carbon fluxes. *Nat. Clim. Chang.* **6**, 1023–1027. <https://doi.org/10.1038/nclimate3114> (2016).
69. Oliphant, A. J. et al. The role of Sky conditions on gross primary production in a mixed deciduous forest. *Agric. Meteorol.* **151**, 781–791. <https://doi.org/10.1016/j.agrformet.2011.01.005> (2011).
70. Saunders, M. et al. Thinning effects on the net ecosystem carbon exchange of a Sitka Spruce forest are temperature-dependent. *Agric. Meteorol.* **157**, 1–10. <https://doi.org/10.1016/j.agrformet.2012.01.008> (2012).
71. Wilkinson, M., Crow, P., Eaton, E. L. & Morison, J. I. L. Effects of management thinning on CO<sub>2</sub> exchange by a plantation oak woodland in south-eastern England. *Biogeosciences* **13**, 2367–2378. <https://doi.org/10.5194/bg-13-2367-2016> (2016).
72. Liu, Q., Sun, Y., Wang, G., Cheng, F. & Xia, F. Short-term effects of thinning on the understory natural environment of mixed broadleaf-conifer forest in Changbai mountain area, Northeast China. *PeerJ* **7**, e7400. <https://doi.org/10.7717/peerj.7400/supp-1> (2019).
73. Binkley, D., Stape, J. L. & Ryan, M. G. Thinking about efficiency of resource use in forests. *Ecol. Manage.* **193**, 5–16. <https://doi.org/10.1016/j.foreco.2004.01.019> (2004).
74. Du, H. et al. Water-use efficiency in a humid karstic forest in Southwestern china: Interactive responses to the environmental drivers. *J. Hydrol.* **617**, 128973. <https://doi.org/10.1016/j.jhydrol.2022.128973> (2023).
75. Xu, Z., Tian, Y., Liu, Z. & Xia, X. Comprehensive effects of atmosphere and soil drying on stomatal behavior of different plant types. *Water* **15**, 1675. <https://doi.org/10.3390/w15091675> (2023).
76. Xu, M. et al. How does thinning affect the photosynthetic parameters and their responses to environmental factors in a subtropical plantation?. *Ecol. Manage.* **595**, 123022. <https://doi.org/10.1016/j.foreco.2025.123022> (2025).

## Acknowledgements

We thank the Data Center of Chinese Terrestrial Ecosystem Flux Observation and Research Network (ChinaFLUX) and the Data Center of Chinese Ecosystem Research Network (CERN) for providing data for this study. We thank Yuanfen Huang, Shanyuan Yin, and Jianzhong Zhang for conducting thinning in the field.

## Author contributions

Conceptualization: Mingjie Xu and Tao Zhang; Methodology: Shengtong Li and Mingjie Xu; Formal analysis: Shengtong Li, Mingjie Xu and Tao Zhang; Investigation: Fengting Yang, Chuanpeng Cheng and Jianlei Wang; Writing - original draft preparation: Shengtong Li and Mingjie Xu; Writing - review and editing: Tao Zhang and Mingjie Xu; Funding acquisition: Mingjie Xu; Resources: Huimin Wang and Fengting Yang; Supervision and project administration: Huimin Wang; Visualization: Jiaxin Song, Xinyi Shi and Ziyi Wang; Data curation: Xianjin Zhu; Software: Shengtong Li.

## Funding

This study was funded by the National Natural Science Foundation of China (grant number 42175141).

## Declarations

## Competing interests

The authors declare no competing interests.

## Additional information

**Correspondence** and requests for materials should be addressed to M.X., H.W. or T.Z.

**Reprints and permissions information** is available at [www.nature.com/reprints](http://www.nature.com/reprints).

**Publisher's note** Springer Nature remains neutral with regard to jurisdictional claims in published maps and institutional affiliations.

**Open Access** This article is licensed under a Creative Commons Attribution 4.0 International License, which permits use, sharing, adaptation, distribution and reproduction in any medium or format, as long as you give appropriate credit to the original author(s) and the source, provide a link to the Creative Commons licence, and indicate if changes were made. The images or other third party material in this article are included in the article's Creative Commons licence, unless indicated otherwise in a credit line to the material. If material is not included in the article's Creative Commons licence and your intended use is not permitted by statutory regulation or exceeds the permitted use, you will need to obtain permission directly from the copyright holder. To view a copy of this licence, visit <http://creativecommons.org/licenses/by/4.0/>.

© The Author(s) 2026